Adsorption 11: 271–277, 2005

Probing the Origins of Linear Free Energy Relationships with Molecular Theory and Simulation

DAVID M. FORD
Department of Chemical Engineering, Texas A&M University, College Station, TX 77843-3122, USA
D-Ford@chemail.tamu.edu

Abstract. Linear free energy relationships (also known as entropy-energy compensation) are seen in a range of physical processes, including adsorption and diffusion. The most interesting compensation effects presumably arise from geometric and energetic effects at the molecular level, but their origins are not well understood. We utilize molecular modeling of simple adsorbate-adsorbent systems to discover these origins in a semi-quantitative way. Sets of calculations were constructed to represent certain experimental processes, e.g. adsorption of a homologous series of molecules, for which linear free energy relationships might be expected. We find that the general correlation between energy and entropy is often much more complex than a simple linear relationship, although a linear approximation might be sufficient across limited ranges.

Keywords: linear free energy relationship, entropy-enthalpy compensation, molecular simulation, adsorption

1. Introduction

In thermodynamics, chemical and physical changes are typically described in terms of free energy changes, such as

$$\Delta A = \Delta E - T\Delta S \tag{1}$$

where A is the Helmholtz free energy, E is the energy, and S is the entropy. This relationship is derived from the first and second laws of thermodynamics and thus has a solid grounding in first-principles theory.

In certain types of physical and chemical processes, researchers have consistently observed a linear relationship between the energetic and entropic contributions to the free energy, as

$$\Delta E = a + b\Delta S \tag{2}$$

where a and b are constants. This so-called linear free energy relationship (LFER) has no grounding in first-principles theory, but it has nevertheless been observed experimentally in widely varied classes of physicochemical processes, sometimes under different names (e.g. isoequilibrium effect, enthalpy-entropy compensation). A recent comprehensive review paper (Liu and Guo, 2001) summarizes the different fields in which LFERs have been observed and current thoughts on their interpretation. Of particular interest here is that LFERs have been observed in adsorption (Denayer et al., 1998; Ruthven and Kaul, 1998; Rudzinski et al., 2000) and diffusion (Fletcher and Thomas, 2000) of small molecules in microporous materials and polymers (Freeman, 1999).

The purpose of this paper is to explore the possible origins of LFERs with molecular modeling techniques. The next section describes the basic molecular model, the necessary concepts in statistical mechanics and links to macroscopic observables, and the calculation procedure. Section 3 contains results for three different "processes" which might be expected to produce a LFER. Section 4 summarizes our conclusions.

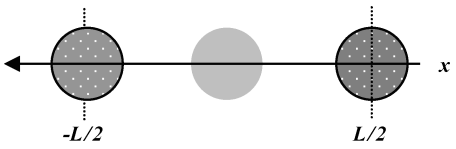

Figure 1. One-dimensional model of an adsorbate in a pore.

2. Model and Theory

2.1. Model

Our simple conceptual model for an adsorbate in a pore is shown in Fig. 1. One atom of the adsorbent is fixed at each of the two endpoints of the pore, $-L/2$ and $L/2$, so that the site has length L. The adsorbate molecule samples the interior of the pore as set by those bounds; the internal structure of the adsorbate molecule is not considered.

The adsorbate molecule is assumed to interact with each adsorbent atom through a Lennard-Jones (LJ) potential such that the total potential energy is

$$\frac{u(x)}{\varepsilon} = 4\left\{\left(\frac{1}{\frac{x}{\sigma}-\left(-\frac{1}{2}\frac{L}{\sigma}\right)}\right)^{12} - \left(\frac{1}{\frac{x}{\sigma}-\left(-\frac{1}{2}\frac{L}{\sigma}\right)}\right)^{6} + \left(\frac{1}{\left(\frac{1}{2}\frac{L}{\sigma}\right)-\frac{x}{\sigma}}\right)^{12} - \left(\frac{1}{\left(\frac{1}{2}\frac{L}{\sigma}\right)-\frac{x}{\sigma}}\right)^{6}\right\} \quad (3)$$

where ε and σ are the LJ parameters describing the adsorbate-adsorbent (i.e. cross) interaction. Figure 2 shows the potential energy function for three different pore sizes.

The potential energy profiles behave as expected from the literature on van der Waals interactions in pores (Derouane et. al., 1988), with two distinct minima at larger pore sizes that merge into a single minimum as the pore gets smaller. The two local wells in the largest pore, $L/\sigma = 5.0$, are each 1.0 ε deep. The next smaller pore, $L/\sigma = 2.245$, has the deepest possible single minimum at 2.0 ε below zero. As we proceed to the smallest pore, $L/\sigma = 2.0$, the single well structure persists but is raised at all locations due to "overlaps" with the solid atoms; the potential energy is always greater than or equal to zero for this pore size.

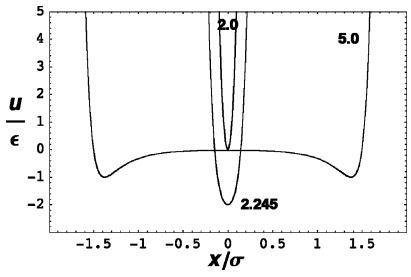

Figure 2. Potential energy of an adsorbate molecule in the model pore, as given by Eq. (3), for three different pore sizes L/σ.

2.2. Theory

2.2.1. Statistical Mechanics. We utilize classical statistical mechanics in our approach; quantum effects are ignored. The key components of this study are the Helmholtz free energy A, energy E, and entropy S of a single adsorbate molecule in the model pore.

Through statistical mechanics (McQuarrie, 1976), we can relate the Helmholtz free energy to a canonical partition function Q as

$$A = -k_B T \ln Q \quad (4)$$

For our model, the canonical partition function may be factored into ideal and excess contributions as

$$Q = (Q^{id})(Q^{ex}) = \left(\frac{L}{\Lambda}\right)\left(\frac{1}{L}\int_{-L/2}^{L/2} e^{-\beta u(x)} dx\right) \quad (5)$$

where Λ is the thermal deBroglie wavelength of the adsorbate molecule and $\beta = 1/k_B T$, with k_B the Boltzmann constant and T the temperature. The excess contribution Q^{ex} reduces to unity when the interaction between the adsorbate and the solid atoms is turned off, i.e. when $u(x) = 0$. It follows that the Helmholtz free energy also has ideal and excess contributions

$$\begin{aligned} A^{id} &= -k_B T \ln Q^{id} \\ A^{\text{ex}} &= -k_B T \ln Q^{\text{ex}} \end{aligned} \quad (6)$$

where $A = A^{id} + A^{\text{ex}}$. The energy E may also be split into two parts as

$$E = K + U \quad (7)$$

where K is the ideal (kinetic) contribution that takes the value $(1/2)k_B T$ for our classical one-dimensional model system, and U is the average potential energy given by

$$U = \frac{\int_{-L/2}^{L/2} u(x) e^{-\beta u(x)} dx}{\int_{-L/2}^{L/2} e^{-\beta u(x)} dx} \quad (8)$$

Finally, the entropy may also be written in two parts as

$$S^{id} = -(A^{id} - K)/T$$
$$S^{\text{ex}} = -(A^{ex} - U)/T \tag{9}$$

where $S = S^{id} + S^{\text{ex}}$.

We will primarily be concerned with correlations between the potential energy U and the excess entropy S^{ex} arising from this model, for reasons discussed in the next section.

2.2.2. Connection with Macroscopic Observables. In the experimental literature, the energetic and entropic components of certain macroscopic properties are obtained and analyzed for LFERs. We demonstrate here that the most relevant properties from our molecular-level model, for the purposes of comparison with the experimental literature, are actually the excess (in the statistical mechanical sense) properties.

As one example, Ruthven and Kaul (1998) found a linear relationship between the entropic and energetic components of the Henry constants for a series of linear paraffins. In the context of our model, the Henry constant for the Gibbs surface excess (in the macroscopic sense) adsorption may be written (Myers, et. al., 1997) as

$$\begin{aligned} K &= \beta \int_{-L/2}^{L/2} \left(e^{-\beta u(x)} - 1\right) dx \\ &= \beta L(Q^{\text{ex}} - 1) \\ &= \beta L(\exp[-\beta A^{\text{ex}}] - 1) \end{aligned} \tag{10}$$

The excess Helmholtz free energy of the adsorbed molecule is clearly the key quantity in the Henry constant, and its components (potential energy and excess entropy) were the quantities plotted by Ruthven and Kaul.

Another example is the diffusion constant in an activated diffusion process. The hopping rate of a molecule from one local free energy basin to another, through a dividing surface, may be expressed (Vineyard, 1957) as

$$k^{\text{TST}} = (2\pi\beta m)^{-1/2} \frac{a Q_a^{\text{ex}}}{v Q_v^{\text{ex}}} \tag{11}$$

in the transition-state theory (TST) approximation. The excess partition function in the numerator is over the area a of the dividing surface and that in the denominator is over the volume v of the basin in which the molecule originates. In the context of our model (Fig. 1), when the two adsorbent atoms are close together, the region between them might be considered as a one-dimensional dividing surface across which a molecule must pass while traveling in a direction normal to the x-axis. The TST hopping rate, which is generally proportional to the macroscopic diffusion constant, is obviously comprised of the ratio of two excess free energies. The relevant energetic and entropic components of a diffusion coefficient (Freeman, 1999) or a mass uptake rate (Fletcher and Thomas, 2000) are therefore actually potential energy and excess entropy.

Based on the foregoing analysis, we believe that a genuine LFER between energetic and entropic components of a macroscopic property should generally be reflected in an LFER between the *potential energy* and *excess entropy* associated with that property. Thus we will focus on excess properties in this work.

2.3. Calculations

Computationally, we obtain A^{ex} from Eqs. (5) and (6), U from Eq. (8), and S^{ex} by subtraction using Eq. (9). All calculations were done in the computational package *Mathematica*® (Version 4.2 for Macintosh). The necessary integrals were actually evaluated to within a small distance ($0.4\,\sigma$) of each endpoint to avoid numerical problems with the divergence of $u(x)$.

3. Results

Next, we focus on the relevant property calculations and possible existence of LFERs during three different "processes" that correspond to perturbing certain experimental parameters. The first process is changing the size of the pore, the second is changing the strength of the adsorbate-adsorbent interaction, and the third is changing the adsorbate species in a homologous series. The results are presented and discussed in the following subsections.

3.1. Changing Pore Size

The first process that we consider is changing the pore size while holding everything else constant. Figure 3 contains the graphs of relevant excess properties as functions of L/σ, as well an entropy-energy parametric plot.

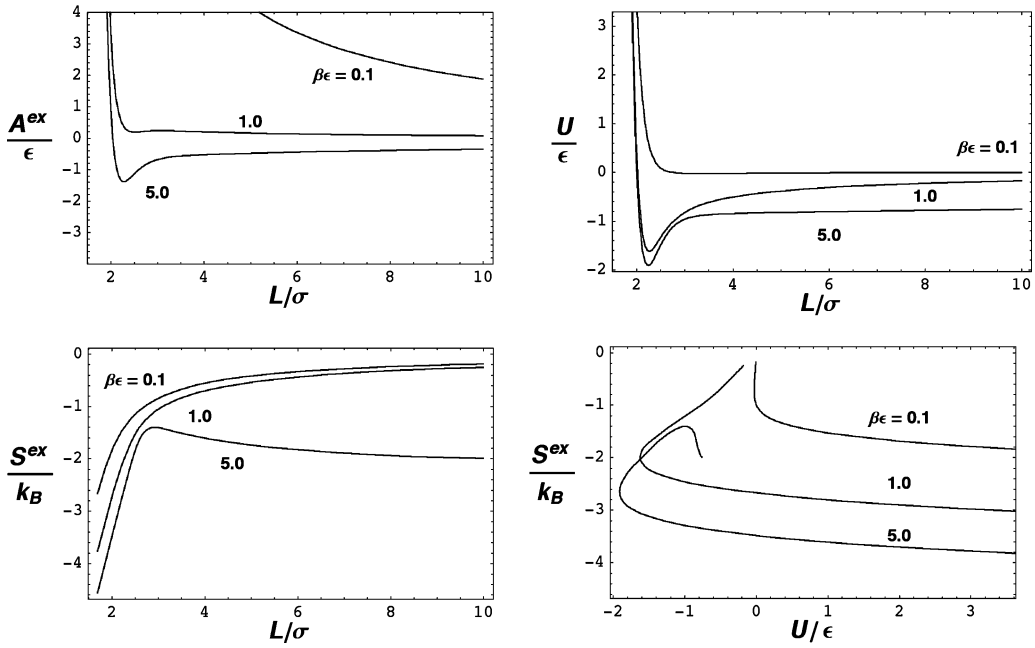

Figure 3. Excess free energy, potential energy, and excess entropy as functions of pore size, and a parametric plot of excess entropy vs. potential energy. The curves are labeled with the corresponding values of $\beta\varepsilon$.

First we discuss the behavior of the individual thermodynamic properties. At the smallest ratio of adsorbate-adsorbent interaction strength to thermal energy, $\beta\varepsilon = 0.1$, the adsorbate does not spend much time sampling the potential energy wells so U is near zero, except for very small pores where it becomes high due to repulsive interactions. The entropy monotonically decreases with decreasing pore size. The overall result is that the free energy is always positive (unfavorable to adsorption), becoming more so as L/σ decreases. The same qualitative trend in free energy is seen for an interaction strength equal to the thermal energy, $\beta\varepsilon = 1.0$, although U takes on negative values in this case and thus reduces the free energy values across all pore sizes. For $\beta\varepsilon = 5.0$, the excess free energy has negative (favorable to adsorption) values for most pore sizes. Under these conditions, the potential energy contribution is dominant, and the adsorbate is highly localized in the favorable potential wells (-1.0 ε for the "separated wells" in large pores and -2.0 ε for the lowest well at $L/\sigma = 2.245$). The behavior of the entropy is very interesting in this case. Starting from a large pore, entropy actually increases slightly as L/σ decreases, until 2.6 or so, where it reaches a maximum before falling with further decrease in L/σ. This interesting non-monotonic behavior is due to the changing structure of the energy wells. For large pores, the adsorbate is localized in one of the two individual wells. As L/σ is lowered, the wells begin to merge together and the energy in the middle of the pore becomes lower. This effectively increases the fraction of the pore length that is accessible to the adsorbate and thus increases the entropy. However, further reduction in L/σ eventually reduces the region available to the adsorbate and entropy falls sharply.

Next we consider the parametric plot of excess entropy *vs.* potential energy. The left-most ends of the curves correspond to the largest L/σ values, while the right-most ends correspond to the smallest L/σ. One obvious feature is that the curves are not linear; the slope changes sign as well as magnitude across the range of L/σ. However, linear approximations would appear to be appropriate for certain limited regions. For the cases where adsorption would be considerable ($\beta\varepsilon = 1.0$ or 5.0 and large L/σ), there is a significant region of positive slope; as the adsorption energy gets stronger, the adsorption entropy decreases. This trend agrees qualitatively with the adsorption data of Ruthven and Kaul (1998). (The $\beta\varepsilon = 5.0$ data has a small tail where the slope becomes negative for large L/σ; this is due to the interesting behavior of excess entropy with pore size as described above.) In the limit of

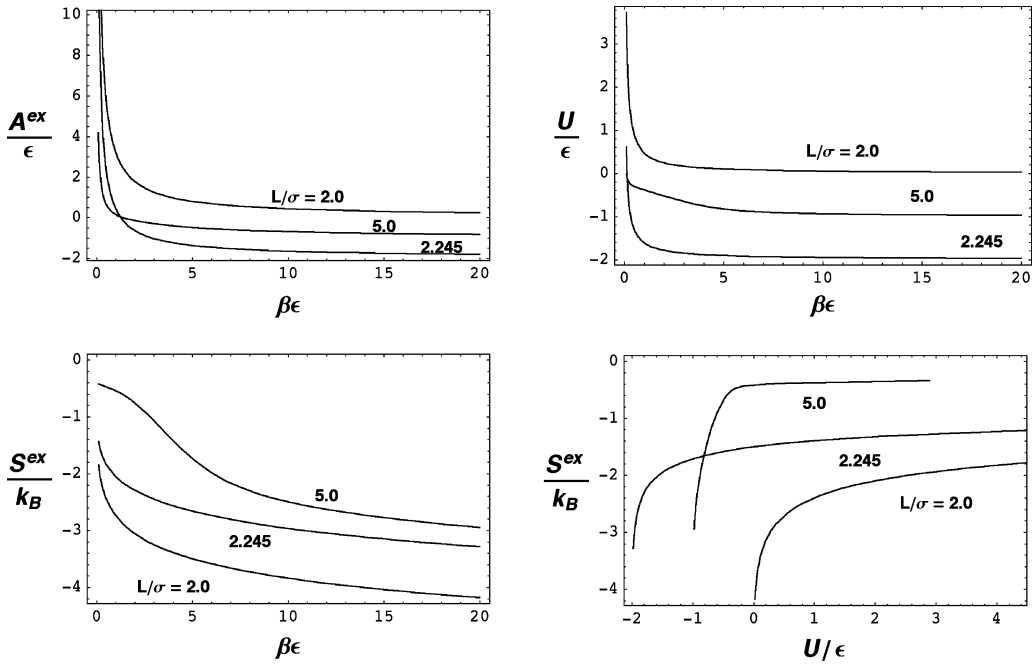

Figure 4. Excess free energy, potential energy, and excess entropy as functions of adsorption strength, and a parametric plot of excess entropy vs. potential energy. The curves are labeled with the corresponding values of L/σ.

small pores, the slope of the curves is always negative; potential energy rises and excess entropy decreases as the pore size is reduced. This limit may be reflective of barriers in activated diffusion processes.

3.2. *Changing Adsorbate-Adsorbent Interaction Energy*

The next process that we consider is changing the strength of the adsorbate-solid interaction while holding everything else constant. Figure 4 contains the graphs of relevant excess properties as functions of $\beta\varepsilon$, as well as an entropy-energy parametric plot. The range of $\beta\varepsilon$ is [0.1, 20] on all plots.

The behavior of the individual thermodynamic properties is straightforward in this process. The excess free energy, potential energy, and excess entropy all decrease monotonically as the interaction strength ε increases. For the smallest pore, the potential energy and excess free energy are always greater than zero, as expected. The free energy curves for the medium and largest pores intersect each other near $\beta\varepsilon = 1.0$; this represents a crossover between entropic and energetic dominance.

Next we consider the parametric plot of excess entropy *vs.* potential energy. The left-most ends of the curves correspond to the largest $\beta\varepsilon$ values, while the right-most ends correspond to the smallest $\beta\varepsilon$. These curves are clearly not linear across the entire range of $\beta\varepsilon$. However, they have positive slope everywhere and each curve appears to have two distinct regions that might be approximated as linear. The region of strong adsorbate-solid interaction has a very steep slope, much steeper in fact than the regions of positive slope seen in the "changing pore size" process of Fig. 3. Thus we conclude that entropy loss due to "energetic confinement" is a strong effect.

3.3. *Adsorption of a Homologous Series of Molecules*

Finally, we consider a process based on the adsorption of a homologous series of molecules into a microporous material. We choose low-molecular-weight n-alkanes as the adsorbates, and zeolite as the adsorbent, in order to compare with the experiments of Ruthven and Kaul (1998). Our model is still the simple one shown in Fig. 1. We use a single LJ interaction site model, not

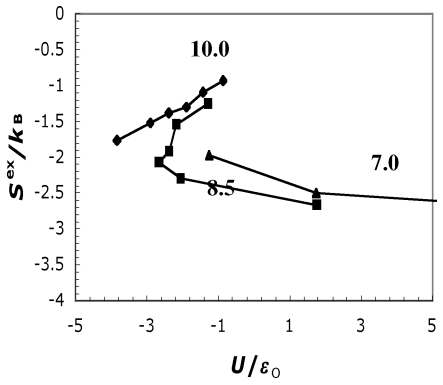

Figure 5. Entropy-energy plot for adsorption of a series of homologous hydrocarbons. The line segments are a guide to the eye. Each data set is labeled with the corresponding value of pore size in Angstroms. The potential energy is normalized by the LJ energy parameter for zeolite oxygen. For the 7.0 Å pore, only the C1 and C2 points can be seen on the scale of this plot.

an explicit atom or methyl group model, to represent the adsorbate. The parameters for the solid atoms were chosen to represent oxygen in a zeolite (June et. al., 1990), with $\sigma_O = 2.806$ Å and $\varepsilon_O/k_B = 96.74\ K$. The LJ parameters for the *n*-alkanes (C1-C5 and C7) were obtained from Tee et al. (1966) using the combined viscosity and second virial coefficient data. The effective σ and ε for the interaction between a given adsorbate and a solid atom were calculated from the standard Lorentz-Berthelot mixing rules. Three different pore sizes L were considered: 7.0, 8.5, and 10 Å. The temperature was chosen to be 300 K. Parametric plots of excess entropy *vs*. potential energy for the process of changing the adsorbate species is shown in Fig. 5.

In Fig. 5, the highest-entropy point on each curve is for the C1 (methane) molecule. The data for the largest pore exhibit a nearly linear relationship with a positive slope. This is similar to the behavior seen in the large-pore limit in the parametric plot of Fig. 3 and the experiments of Ruthven and Kaul (1998). However, a linear fit to our data in Fig. 5 yields an inverse slope of 348 K, whereas Ruthven and Kaul found inverse slopes of 970 and 1035 K from their data on silicalite and faujasite, respectively. The substantial disagreement between our results and theirs almost certainly stems from the simplicity of our model; a full-atom model with correct three-dimensional zeolite pore structure would likely be more accurate. The data for the middle-sized pore capture both the positive slope (adsorption) and negative slope (barrier) regimes, as seen in Fig. 3, while the smallest pore is clearly of the barrier type.

4. Conclusions

We employed a simple one-dimensional adsorption model based on van der Waals interactions to examine the origins of LFERs. We demonstrated that potential energy and excess entropy are the key components from the molecular model that would be manifested in a macroscopically observed LFER. We simulated three processes for which an LFER might be expected: changing the pore size of the adsorbent, changing the adsorbate-adsorbent interaction strength, and changing the adsorbate species in a homologous series. In each case, we observed a relationship between excess entropy and potential energy that was more complex than linear. For the processes of changing the pore size and the adsorbent species, the slope of the curves actually changed sign; regions corresponding to favorable adsorption (pore size > molecular size) were characterized by a positive correlation between entropy and energy, while regions corresponding to diffusion barriers (pore size < molecular size) were characterized by a negative correlation. Despite the global complexity in the entropy-energy curves, a linear relationship could be appropriate across limited ranges of parameter space.

References

Denayer, J.F., G.V. Baron, J.A. Martens, and P.A. Jacobs, "Chromatographic Study of Adsorption of n-Alkanes on Zeolites at High Temperatures," *Journal of Physical Chemistry B*, **102**, 3077–3081 (1998).

Derouane, E.G., J.M. Andre, and A.A. Lucas, "Surface Curvature Effects in Physisorption and Catalysis By Microporous Solids and Molecular-Sieves," *Journal of Catalysis*, **110**, 58–73 (1988).

Fletcher, A.J. and K.M. Thomas, "Compensation Effect For The Kinetics of Adsorption/Desorption of Gases/Vapors on Microporous Carbon Materials," *Langmuir*, **16**, 6253–6266 (2000).

Freeman, B.D., "Basis of Permeability/Selectivity Tradeoff Relations in Polymeric Gas Separation Membranes," *Macromolecules*, **32**, 375–380 (1999).

June, R.L., A.T. Bell, and D.N. Theodorou, "Molecular Dynamics Study of Methane and Xenon in Silicalite," *J. Phys. Chem.*, **94**, 8232–8240 (1990).

Liu, L. and Q.-X. Guo, "Isokinetic Relationship, Isoequilibrium Relationship, and Enthalpy-Entropy Compensation," *Chem. Rev.*, **101**, 673–695 (2001).

McQuarrie, D.A., *Statistical Mechanics*. HarperCollins, New York, 1976.

Myers, A.L., J.A. Calles, and G. Calleja, "Comparison of Molecular Simulation of Adsorption With Experiment," *Adsorption-Journal of the International Adsorption Society*, **3**, 107–115 (1997).

Rudzinski, W., T. Borowiecki, T. Panczyk, and A. Dominko, "On The Applicability of Arrhenius Plot Methods to Determine Surface Energetic Heterogeneity of Adsorbents and Catalysts Surfaces From Experimental TPD Spectra," *Advances in Colloid and Interface Science*, **84**, 1–26 (2000).

Ruthven, D.M. and B.K. Kaul, "Compensation Theory of Adsorption: Correlation and Prediction of Henry Constants for Linear Paraffins on Zeolite Adsorbents," *Adsorption-Journal of the International Adsorption Society*, **4**, 269–273 (1998).

Tee, L.S., S. Gotoh, and W.E. Stewart, "Molecular Parameters for Normal Fluids—Lennard-Jones 12-6 Potential," *Industrial and Engineering Chemistry Fundamentals*, **5**, 356 (1966).

Vineyard, G.H., "Frequency Factors and Isotope Effects in Solid State Rate Processes," *J. Phys. Chem. Solids*, **3**, 121–127 (1957).